

Genomic characterization of vulvar squamous cell carcinoma

TEMPUS

Sara R. Selitsky¹, Tasha Thong¹, Kimberly Roche¹, Justin Guinney¹, Praveen Sethupathy², Catherine Igartua¹

¹Tempus AI, Chicago IL

²Department of Biomedical Sciences, College of Veterinary Medicine, Cornell University, Ithaca, NY

Published Abstract Number: 6454

INTRODUCTION

Vulvar squamous cell carcinoma (vSCC) is a rare cancer (Figure 1A) with limited treatment options.

- vSCC has two main causes which confer different prognoses and treatment sensitivity, but are currently treated the same clinically.
 - Human Papillomavirus (HPV) and skin conditions, such as lichen sclerosus.
- Stage III and IV vSCC have poor prognosis, leading to 47% and 23% 5-year survival respectively (Ref: SEER Database).

Squamous cell carcinomas (SCCs) are defined by cancer of the squamous cells, flat cells in the epidermis.

- SCCs have tissue site-independent molecular signatures (Figure 1B).
- SCC treatments are heterogenous, with combinations of chemotherapy and immune checkpoint inhibitors comprising first-line treatment (Figure 1C).

To better understand vSCCs molecularly, we unbiasedly subtyped vSCCs tumors and mapped them to a large cohort of several SCC types.

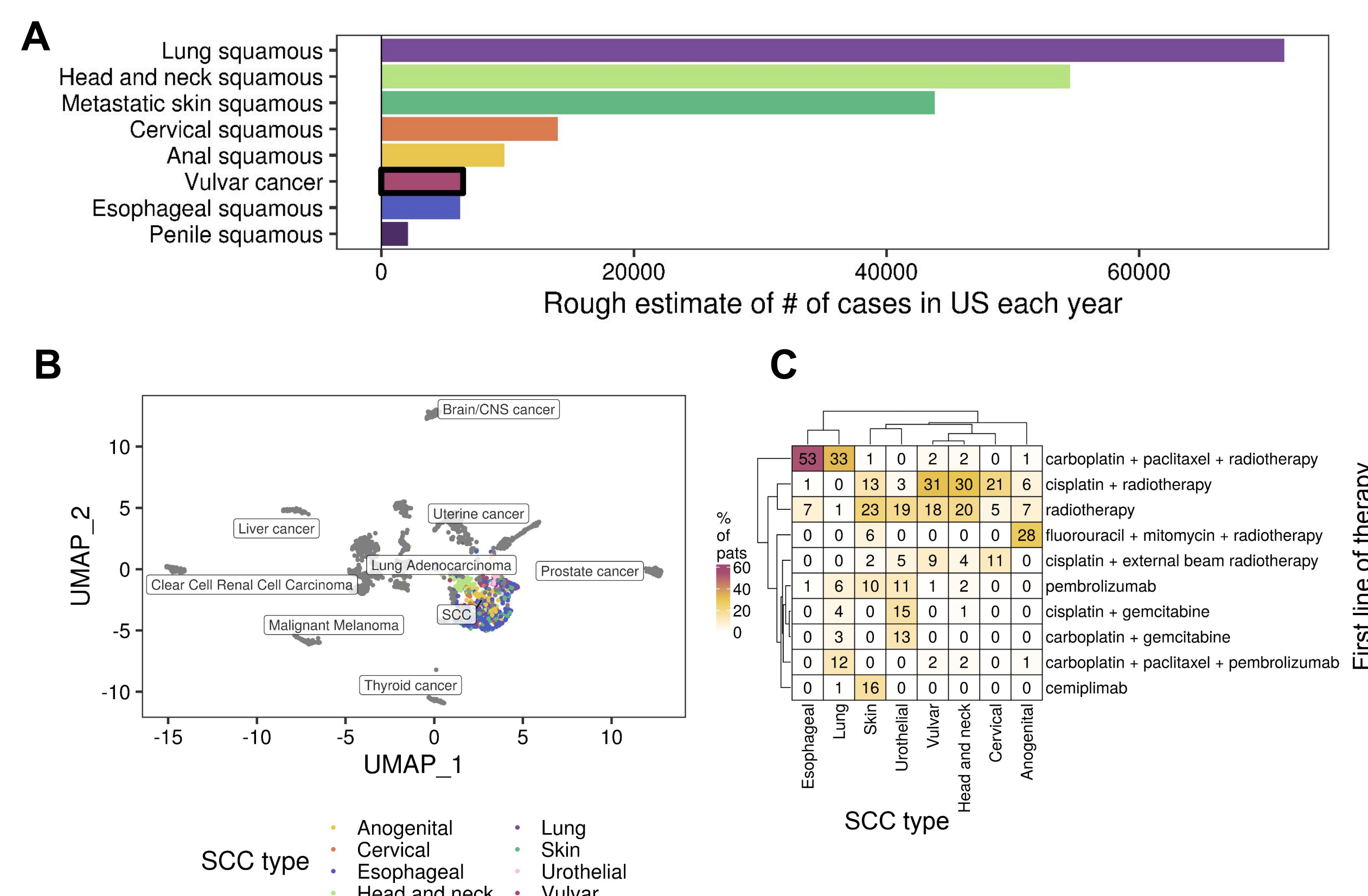


Figure 1. vSCCs may benefit from additional SCC context. (A) Estimate number of new diagnoses for each cancer in the US for each year. (Refs: SEER database when available, Rogers *et al.* JAMA 2015, Cancer.net, Lungevity.org, Then *et al.* World J. Oncol. 2020, Cancer.org) (B) Gene expression UMAP dimension reduction from across 27 different cancer types (n=2,743 samples) from the Tempus database. SCC transcriptomes cluster based on squamous gene-expression rather than by tissue or origin. SCC is plotted in color while non-SCC are represented in gray as a reference. (C) Heatmap of SCC first line therapy treatment frequencies in the Tempus database. Each cell in the heatmap represents the % of samples treated with each therapy for each cancer type.

METHODS

- De-identified SCC records were selected from the Tempus Database (Figure 2).
- Vulvar cancers annotated with squamous histology and available RNA-seq were selected for analysis. Samples derived from lung and liver metastases were excluded from analysis due to the background effect on gene expression.
- The pan-SCC cohort was limited to randomly sampled (for cohorts >100 samples) primary, naive to any treatment, female samples with paired RNA- and DNA-seq from 7 additional SCC types.
 - Pan-SCC cohort: lung (n=100), head and neck (n=100), skin (n=100), uterine (n=49), cervical (n=100), anogenital (n=27), esophageal (n=100), and vSCC (n=273)
- For both cohorts, we performed gene expression-based clustering analysis using FastPG-CC, an internally developed consensus-clustering extension of FastPG (Bodenheimer *et al.* BioRxiv, 2020), a graph-based parallelized clustering tool.

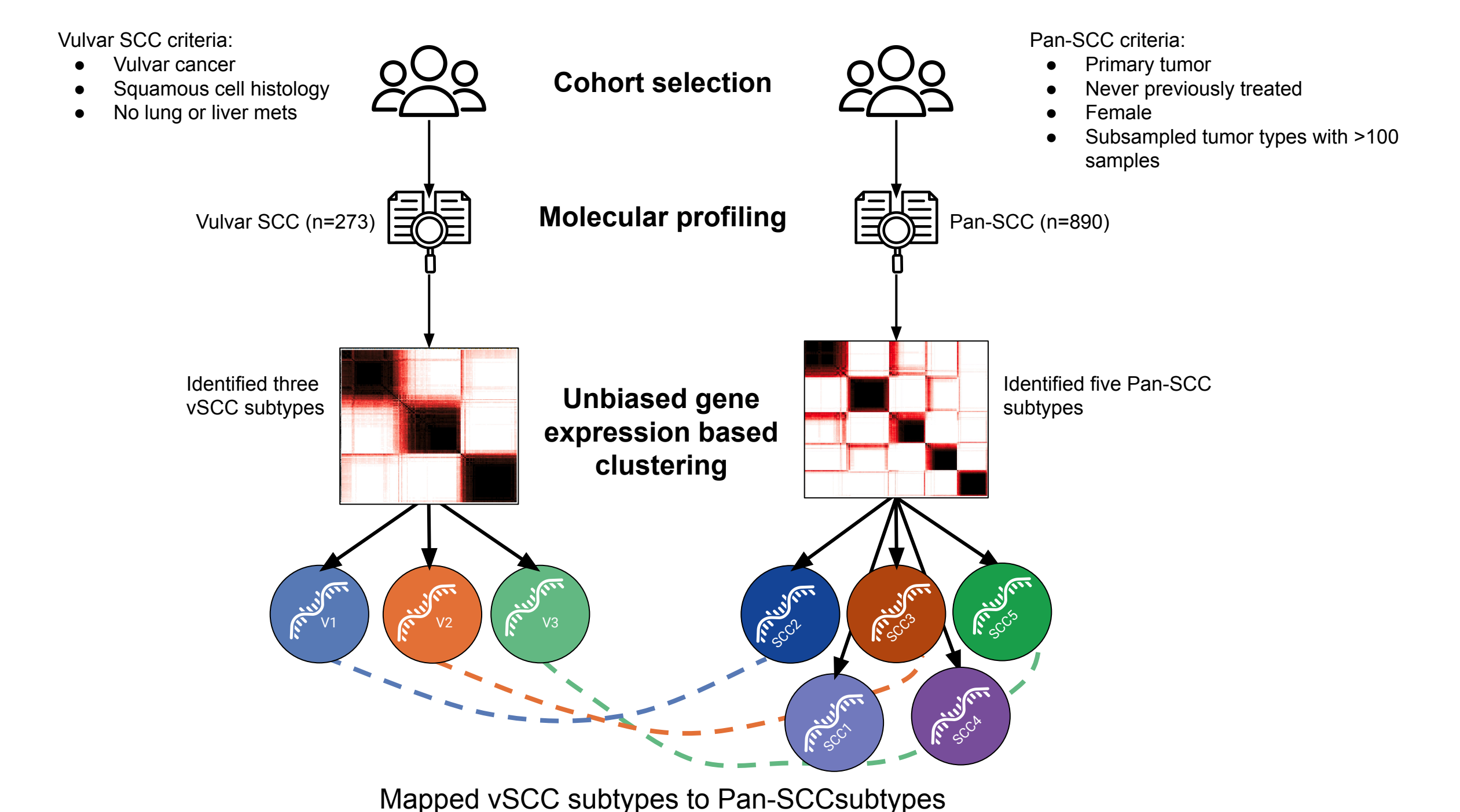


Figure 2. Pictorial representation of the workflow of this analysis.

ACKNOWLEDGMENTS

We thank Matthew Kase, Adam Hockenberry, Alexandria Bobe, and Vanessa Nepomuceno from the Tempus Science Communications team for poster development.

SUMMARY

- Vulvar squamous cell carcinoma (vSCC) splits into three subtypes based on gene expression.
- Each vSCC subtype mapped to a subtype derived from a pan-SCC cohort and gene expression of vSCC was almost indistinguishable from specific SCC types.
- Pan-SCC subtype probabilities were associated with prognosis across all SCCs.

RESULTS

vSCCs in the Tempus clinico-genomic database

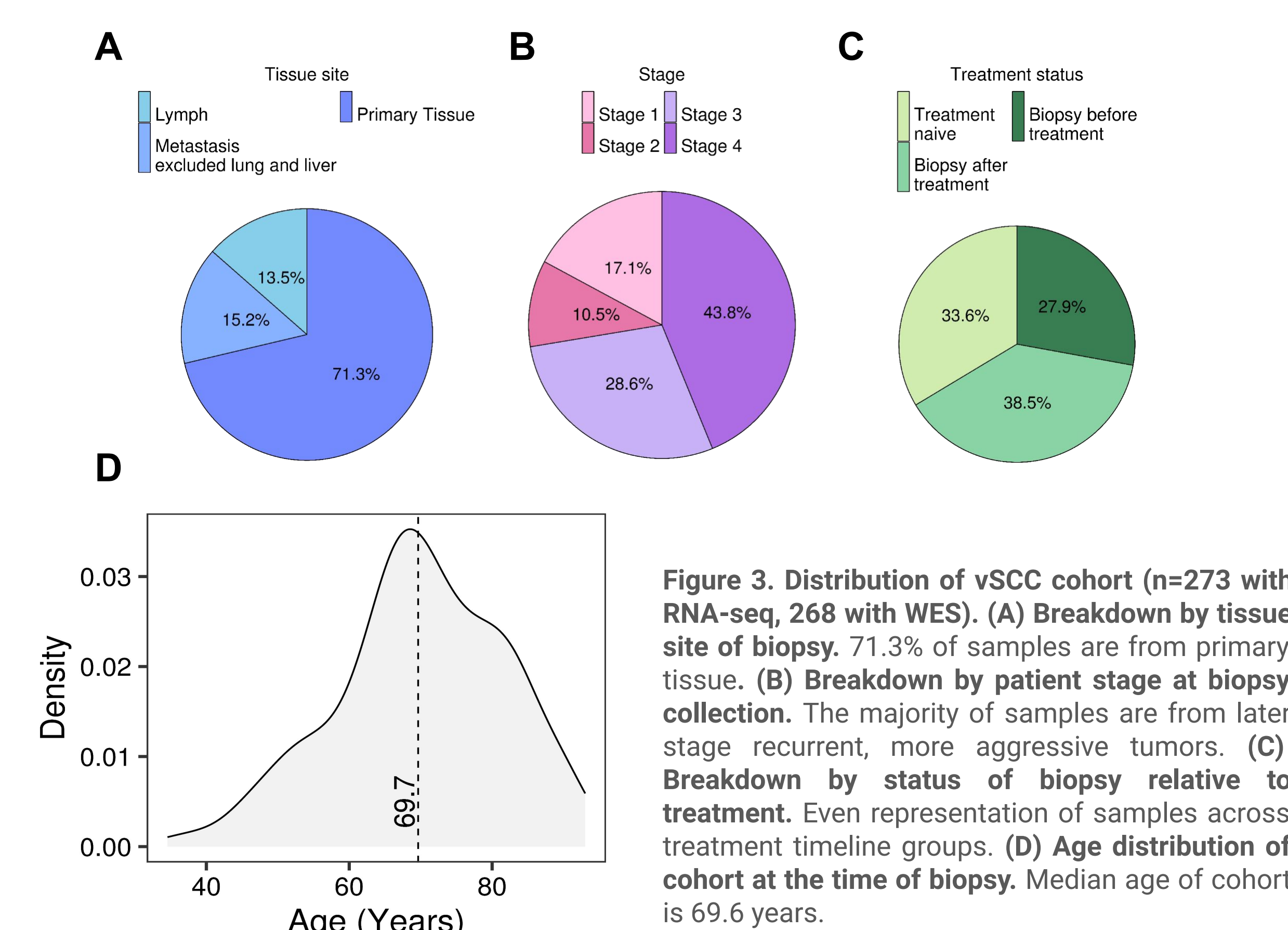


Figure 3. Distribution of vSCC cohort (n=273 with RNA-seq, 268 with WES). (A) Breakdown by tissue site of biopsy. 71.3% of samples are from primary tissue. (B) Breakdown by patient stage at biopsy collection. The majority of samples are from later stage recurrent, more aggressive tumors. (C) Breakdown by status of biopsy relative to treatment. Even representation of samples across treatment timeline groups. (D) Age distribution of cohort at the time of biopsy. Median age of cohort is 69.6 years.

vSCCs alterations stratify by HPV status

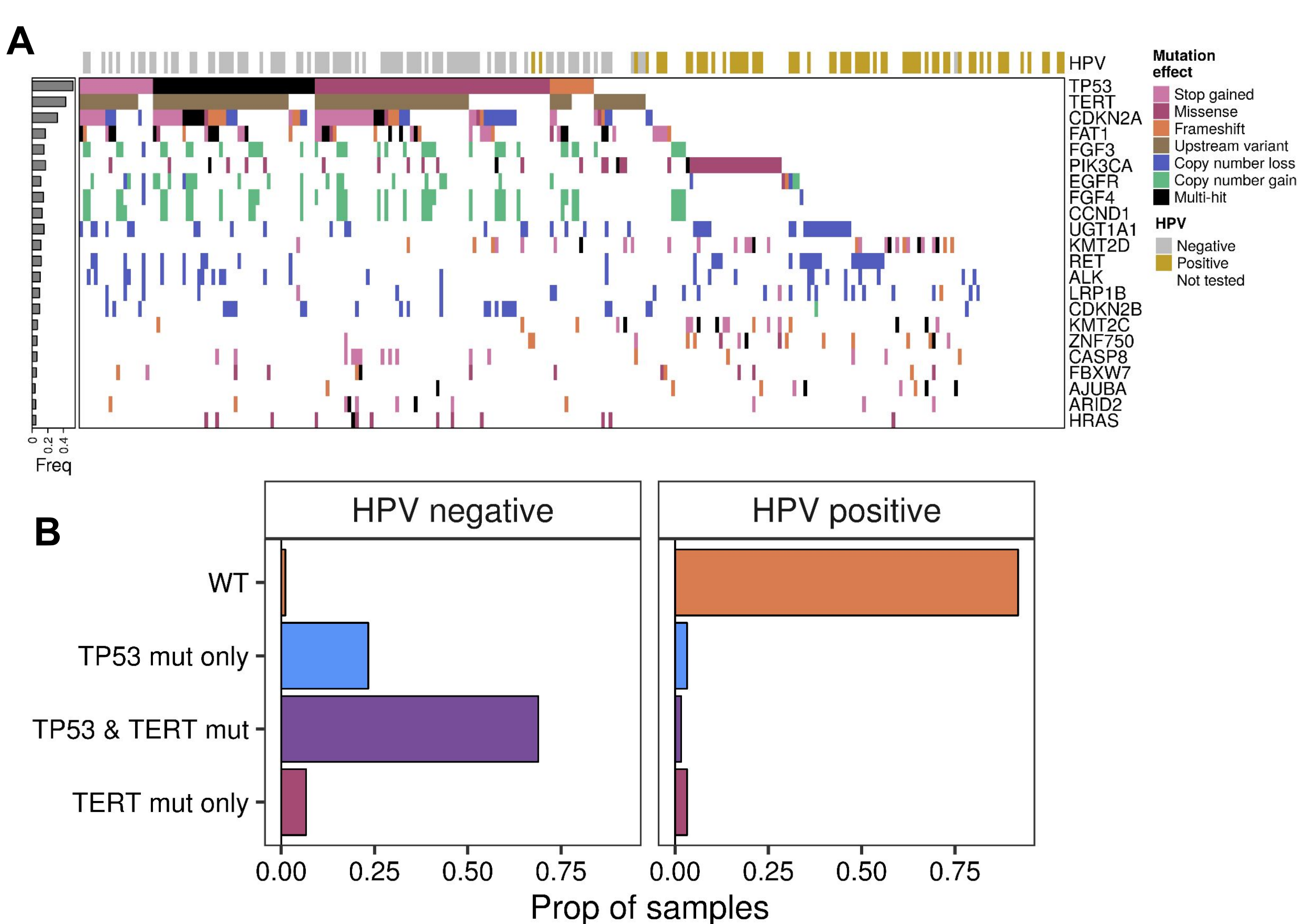


Figure 4. vSCC alterations stratify based on HPV status. (A) Top 20 altered genes in vSCC in reference to HPV status. Somatic pathogenic alterations (mutation and copy number) are represented. Left panel represents somatic mutation frequency of each gene. (B) Co-occurrence frequency of *TP53* and *TERT* mutations by HPV status. HPV calls were present in 57% (152/268) of the samples. *TP53* and *TERT* promoter mutations were enriched in HPV negative samples (98.8% vs. 8%) and are predictive of HPV status with a 97% balanced accuracy.

vSCC split into three subtypes

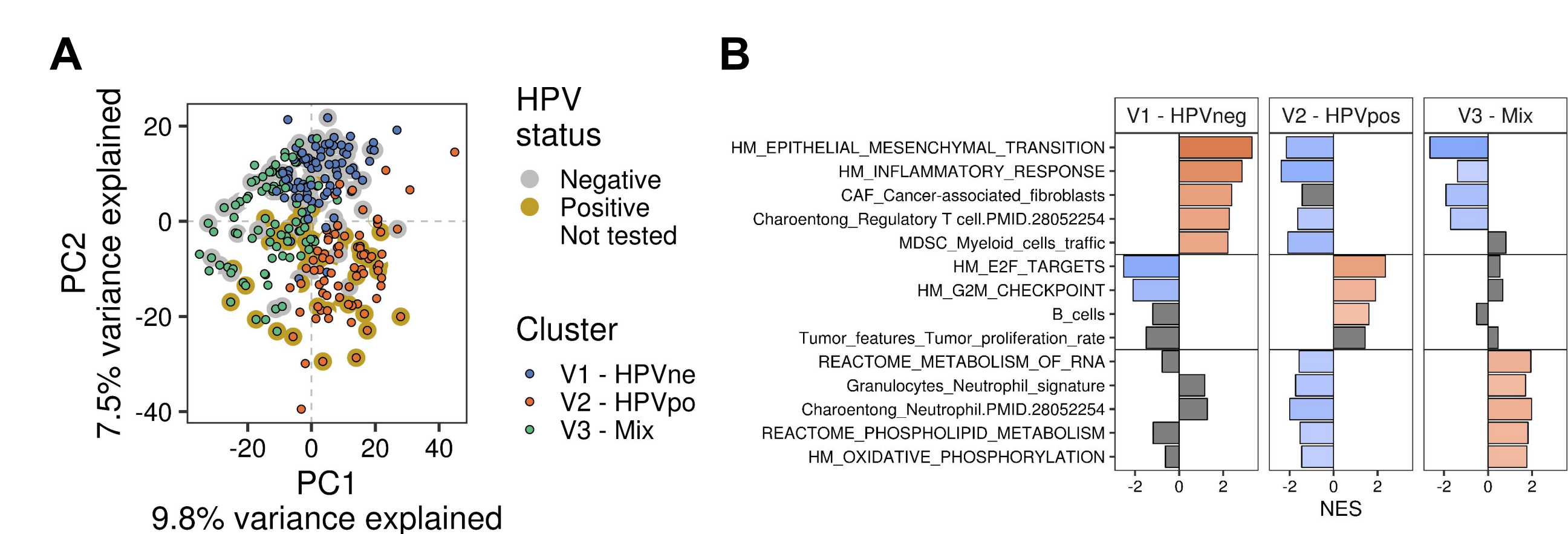


Figure 5. vSCCs split by EMT, immune, and cell cycle features (A) vSCC gene expression principal component analysis (PCA). The largest source of variation (PC1) in this cohort was the split of vSCC subtype V3 vs. the rest, whereas HPV accounted for the second largest source of variation. (B) Gene set enrichment analysis results for each cluster. Linear regression derived beta-coefficients of each cluster vs. the rest, were applied as gene ranks into GSEA. Gene sets displayed represent signatures unique to a subtype. Color of the bar and the x-axis represents the normalized enrichment score, with gray representing no significance (Q>0.1). Unbiased subtyping of the gene expression of the vSCC cohort led to robust subtypes, including V1-HPVneg: mostly HPV negative and *TP53/TERT* mutated (93% and 90%, respectively), characterized by high expression of epithelial to mesenchymal transition (EMT) and a suppressive tumor microenvironment, V2-HPVpos: characterized by HPV positivity (75%), high expression of proliferation and B-cell related genes, and V3-Mix: comprised of both HPV positive and negative (42% positive) samples, characterized by high metabolic and neutrophil expression, and more differentiated.

Head and neck, skin, and vulvar SCCs were heterogeneous based on gene expression

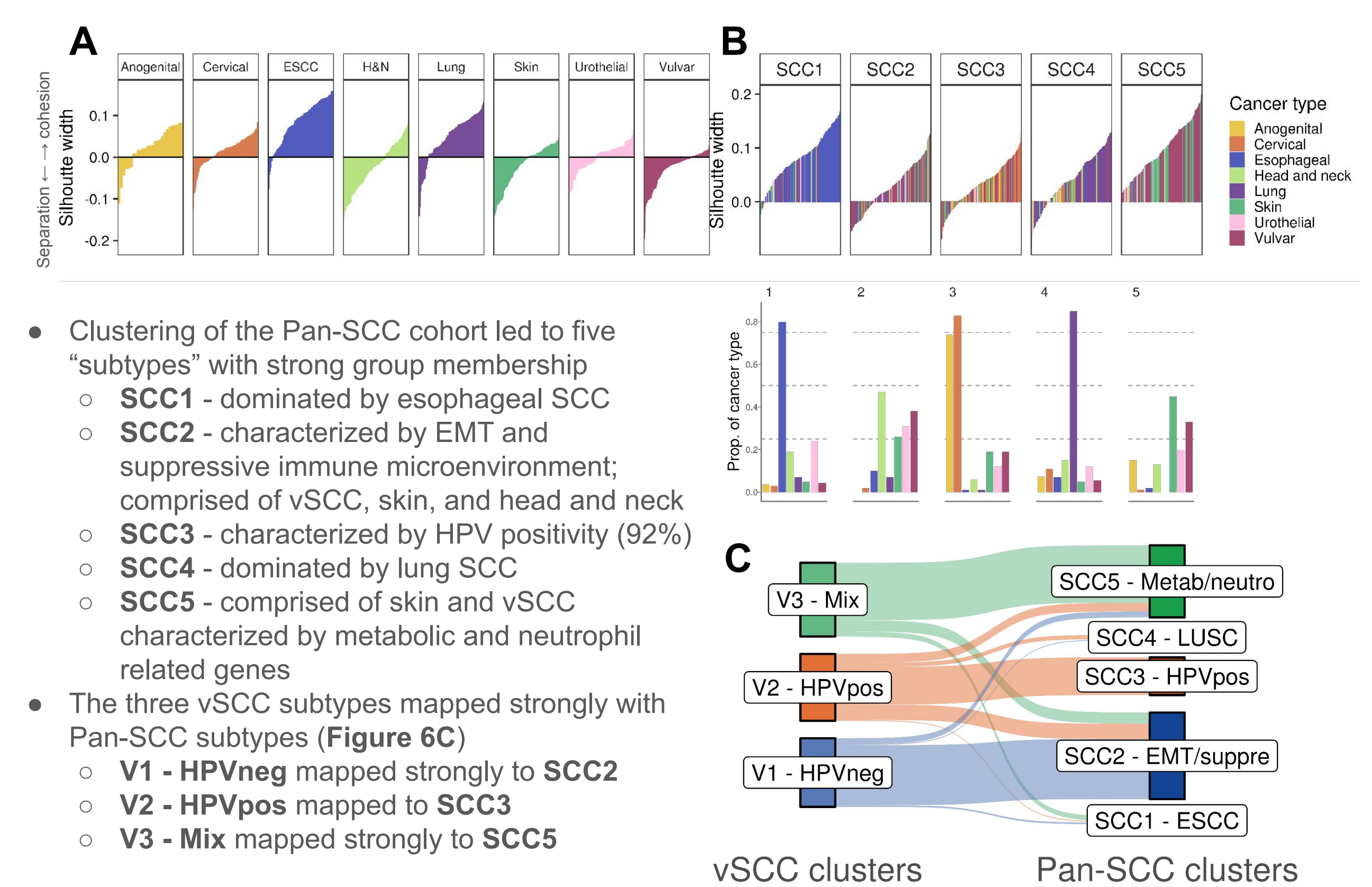


Figure 6. Pan-SCC subtyping leads to robust cluster membership. Lung, cervical, anogenital and esophageal SCCs had strong gene expression-based tissue type cohesion, meaning samples within those cancer types were more similar to each other than to other SCC types. Head and neck, skin, and especially vulvar SCCs were heterogeneous; samples within these tumor types were more similar to other SCC types. Silhouette width (SW) plots that display the cluster cohesion vs. the cluster separation. Higher the value, more strongly the sample belongs to the assigned cluster, while the negative values represent samples which map closer to another tissue. (A) SW results for tissue type; measuring the SW with tissue type as "cluster", (B) Pan-SCC subtype SW plot. Barplot above represents the % of each cancer type belonging to each Pan-SCC subtype. (C) Sankey plot representing the proportion of vSCC samples from each vSCC subtype mapping to each Pan-SCC subtype.

vSCCs were almost indistinguishable from skin SCC by gene expression

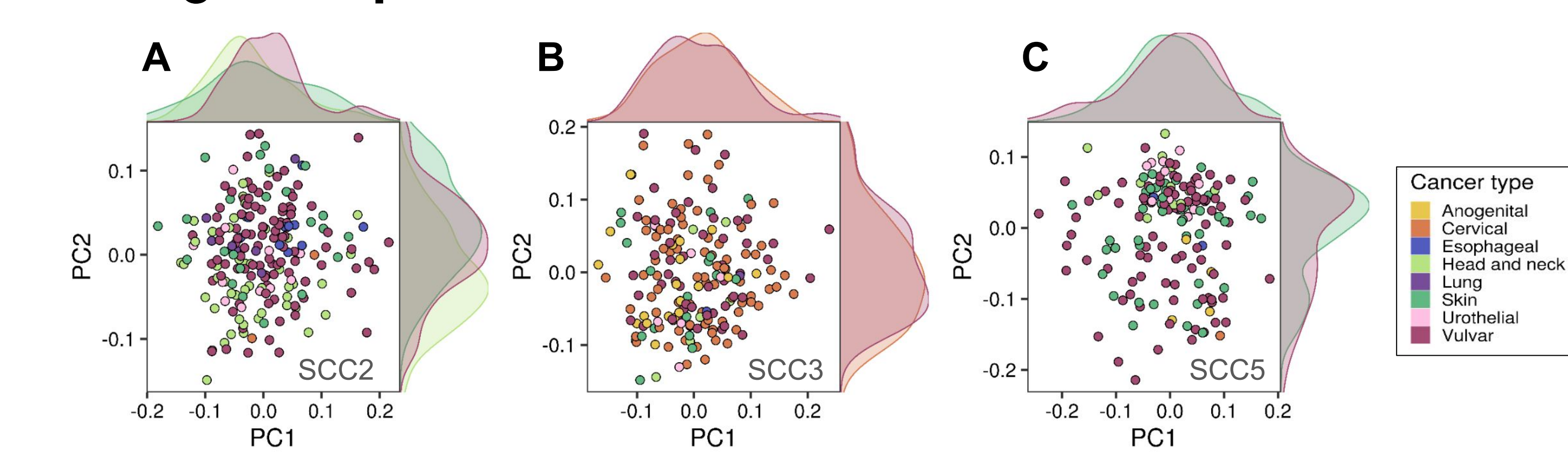


Figure 7. Gene expression analyses of vSCC within SCC subtypes which vSCCs were mostly found in SCC2, 3, and 5 revealed that vSCCs were almost indistinguishable to skin SCC. Within (A) SCC2, vSCCs vs. skin SCC had only 3 differentially expressed genes (DEGs), whereas vSCC vs. head and neck had 193 DEGs, within (B) SCC3, vSCCs vs. cervical cancer had 128 DEGs, and within (C) SCC5, vSCC vs. skin had 11 DEGs. DEG criteria: linear regression, FDR multiple testing correction, Q<0.1. Principal component 1 and 2 for all samples within each Pan-SCC subtype which had >20 vSCC samples. Density plots on the outside of the scatter plots represent the PC1 (x-axis) or PC2 (y-axis) density for cancer types present in >20 samples for each Pan-SCC subtype.

SCC membership was associated with overall survival

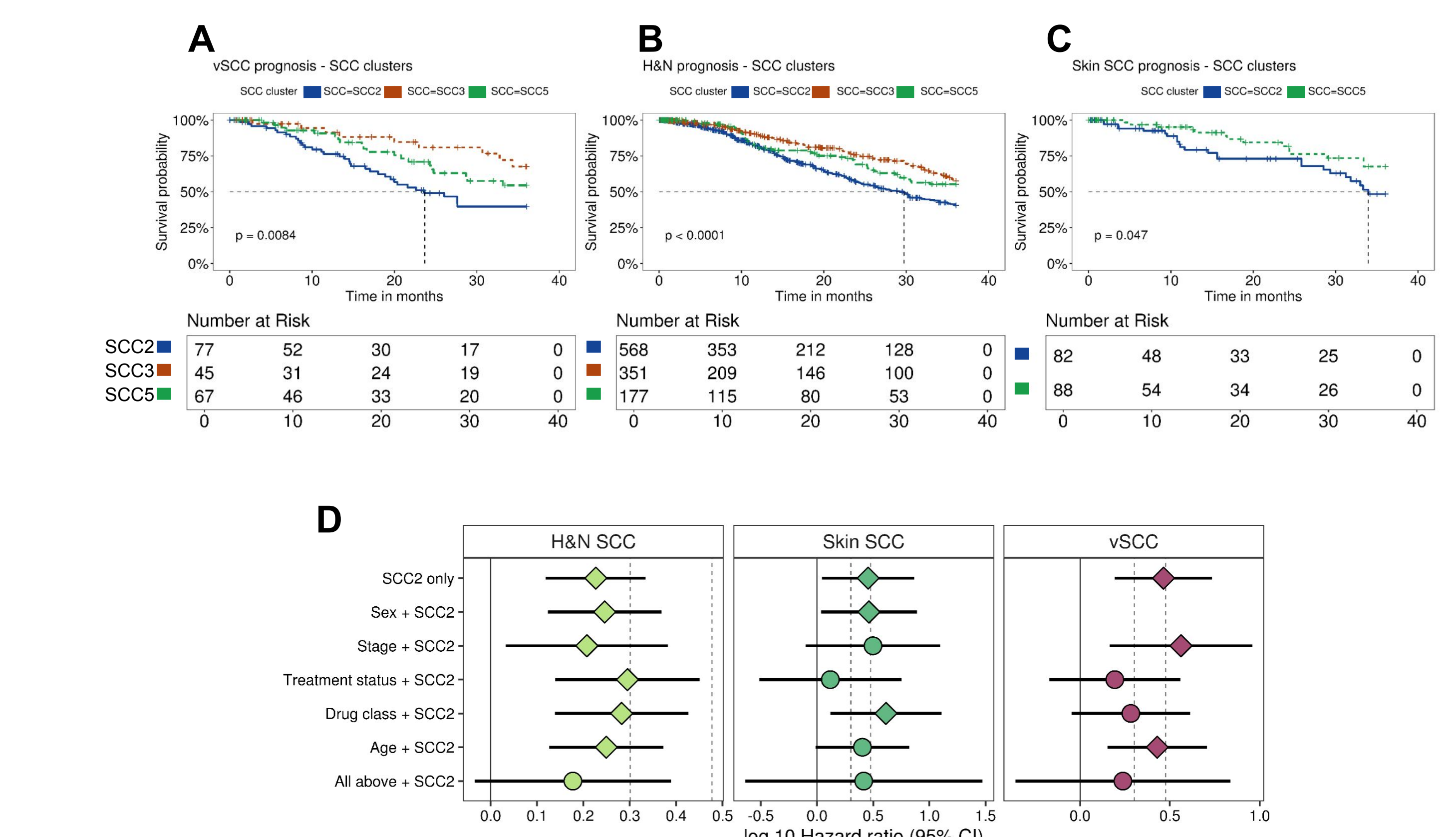


Figure 8. SCC2 assignment and SCC2 probability were both associated with worse OS. Using multinomial elastic net, SCC subtypes were applied to a larger SCC cohort from the Tempus clinico-genomic database (n=7,263) for outcomes analyses. Patients with samples in SCC2 had consistently worse outcomes compared to patients with samples from SCC5 in cancer types with >50 samples in each: vSCC (p = 0.06, HR = 1.7, Cox PH), head and neck (p = 0.01, HR = 1.5), skin squamous (p = 0.05, HR = 1.9) (A-C) Kaplan-Meier plots displaying the overall survival (OS) probability for the cancer types with >50 samples in Pan-SCC2 and SCC5. P-value on plot was determined using Log Rank Test. (D) SCC2 probability was associated with OS after accounting for clinical covariates. Cox proportional hazards association with SCC2 probability only, or SCC2 probability with an additional covariate. "All above" refers to a multivariate model including stage, sex (if not vSCC), treatment status, and age.